Self-Assembly of Metalloporphyrins into Light-Harvesting Peptide Nanofiber Hydrogels for Solar Water Oxidation

Jae Hong Kim, Dong Heon Nam, Yang Woo Lee, Yoon Sung Nam, and Chan Beum Park**

The use of renewable and clean energy is critically needed for the sustainability of our society since fossil fuels cause serious environmental problems.[1,2] Solar energy is undoubtedly a promising energy resource, but its use is limited by the low irradiance intensity (about 100 mW/cm^2), intermittence, and geographical heterogeneity. Photovoltaic systems have intrinsic limitation in solving these problems because of difficulties in the storage and transportation of electrical energy. In nature, solar energy is converted to chemical energy in green plants, algae, and cyanobacteria via photosynthesis. Enormous efforts have been made to develop an artificial photosynthetic system for the production of clean fuels by utilizing solar energy.[3–6] Water-splitting, however, is a highly challenging reaction because it requires multiple-electron transfer coupled with proton transfer at a minimum potential of 0.81 V versus normal hydrogen electrode (NHE) at pH 7 on average for each electron transfer.[7] Photosystems overcome this intrinsic limitation using sophisticated protein scaffolds for the optimization of the spatial arrangement of functional molecules, such as catalytic clusters (i.e., Mn complexes), redox relay molecules (i.e., quinone complexes), and chromophores (i.e., chlorophylls), as illustrated in Figure S1 in the Supporting Information. In particular, a well-defined spatial alignment of chromophores is critically important for efficient excitation energy transfer (EET) to the reaction center, so that photosystems effectively generate a gradient of electrochemical potential for photosynthetic reactions.[8] Thus, it is highly desirable to construct artificial light-harvesting complexes for EET. However, the precise assembly of multiple chromophores with redox catalysts is technically very difficult, imposing limitations to EET for light-driven water-splitting.[9–13]

Herein we report on the application of molecular self-assembly for photochemical water oxidation under visible light. Self-assembled biomolecular nanostructures can serve as a scaffold for the nanoscale arrangement of chromophores to generate a series of Förster-type resonance energy transfer (FRET) events, which increases the delocalization of excitation energy toward catalysts for light-driven water oxidation.[14–17] Among various self-assembling biomolecules, diphenylalanine (Phe-Phe, FF) was chosen because it is the simplest amino acid motif that can produce unique nanostructures with structural flexibility and molecular recognition capability.[18–22] The self-assembled FF nanostructures exhibited unparalleled optical, electrochemical, mechanical properties with high stability and biocompatibility.[23–26] Furthermore, the substitution of diphenylalanine with other amino acids (e.g., glycine) can induce the self-assembly of nanostructures having different properties, demonstrating that the functional set of molecules can be extended simply by the change of amino acids.[27] In this work, we incorporated metalloporphyrins into a rigid and transparent nanofiber network of Fmoc-FF under ambient conditions through an in-situ self-assembly process (**Scheme 1**).[28] The self-assembled Fmoc-FF structure induced the J-aggregation (i.e., face-to-tail arrangement) of the metalloporphyrins, which are found in the core of chlorophyll molecules and have high absorbance in the visible light (Soret band: 0.2 ~ 4 × 10^5 M^{-1} cm^{-1} from 380 to 400 nm, Q-band: 1 ~ 2 × 10^4 M^{-1} cm^{-1} from 500 to 600 nm). The J-aggregation of porphyrins can induce EET between the assembled porphyrins. We chose meso-tetra(4-pyridyl) porphine (TPyP) because it has four pyridyl groups at the meso-functional position, which can interact with the functional groups of Fmoc-FF nanofibers, such as carboxylic and hydroxyl groups. The incorporation of TPyP into the Fmoc-FF nanofibers can be driven through non-covalent interactions (e.g., electrostatic interaction and hydrogen bonding) between the pyridyl group of TPyP and the carboxylic and hydroxyl groups of Fmoc-FF.[28]

To prepare the Fmoc-FF/TPyP hybrid nanofibers, a mixture of Fmoc-FF and TPyP with a molar ratio of 95:1 in 1,1,1,3,3,3-hexafluoro-2-propanol (HFIP) was 50-times diluted with deionized water. Three types of TPyP monomers (H2TPyP, ZnTPyP, and SnTPyP) having different metal centers were tested to determine the effects of coordinated metal ions on the incorporation of the porphyrins into Fmoc-FF nanofibers. All of the mixtures of Fmoc-FF and TPyP spontaneously formed a self-standing hydrogel, and no apparent difference

J. H. Kim, D. H. Nam, Y. W. Lee, Prof. Y. S. Nam, Prof. C. B. Park
Department of Materials Science and Engineering
Korea Advanced Institute of Science and Technology
335 Science Road, Daejeon, 305–701,
Republic of Korea
E-mail: yoonsung@kaist.ac.kr; parkcb@kaist.ac.kr

DOI: 10.1002/smll.201302627

NANO MICRO small

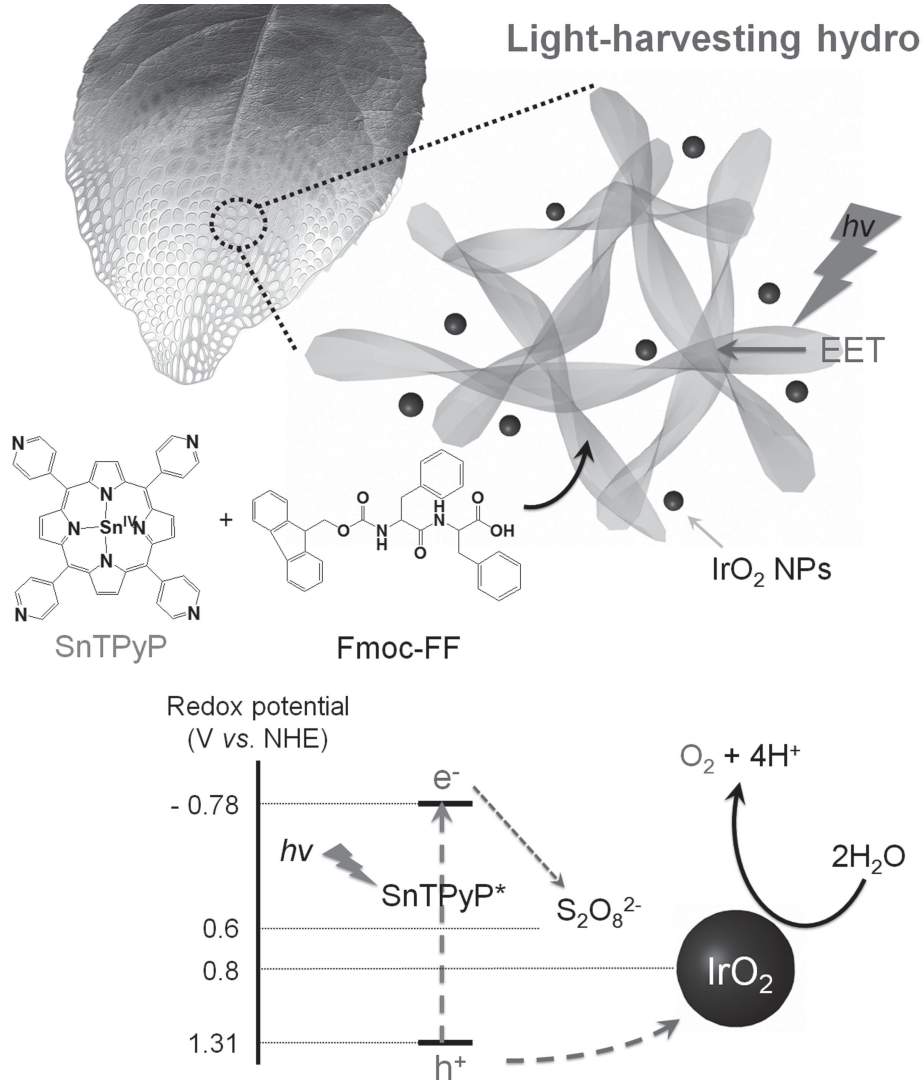

Scheme 1. Schematic illustration of visible light-driven water oxidation by self-assembled light-harvesting hydrogel. The self-assembled hydrogel was incorporated with metalloporphyrins having oxidation and reduction potentials of 1.31 V and −0.78 V vs. Ag/AgCl, respectively, for light-driven water oxidation catalyzed by iridium oxide catalysts. The impact of the self-assembly of the chromophores on photocatalysis is investigated in this work.

was observed except for their intrinsic colors (Figure S2). The amount of TPyP molecules eluted from the Fmoc-FF/TPyP hydrogels (Figure S3) was negligible, indicating the successful incorporation of the TPyP molecules into the Fmoc-FF hydrogel. The electron microscopic images of the Fmoc-FF hydrogel with and without TPyP showed that the incorporation of TPyP molecules did not affect the morphology of the Fmoc-FF nanofibers (**Figure 1**A,B and Figure S4); this result suggests that TPyP did not disturb the inherent structure of the Fmoc-FF hydrogel. It was also confirmed that the intrinsic β-sheet structure of the Fmoc-FF hydrogel, generated from π-π interaction between the Fmoc-FF molecules, was maintained after the incorporation of the porphyrins into the Fmoc-FF hydrogel, using Fourier transform infrared (FT-IR) spectroscopy, fluorescence spectroscopy, and wide-angle X-ray scattering analysis (Figure S5 and S6).[28] The surface of the Fmoc-FF hydrogel has carboxylic groups that appear regularly along the Fmoc-FF nanofiber.[28] The Fmoc-FF nanofibers are negatively charged at a neutral pH because of the deprotonation of the carboxylic group having a pKa of ≈6.[29] On the other hand, HFIP facilitates the dissolution of TPyP (pKa ~ 4.76)[30] by the protonation of pyridyl groups,[31] as shown in Figure S7. A gradual dissociation of TPyP from the hydrogel was observed when 0.1 M HCl was added to the Fmoc-FF/TPyP hydrogels to promote the protonation of the carboxylic group of Fmoc-FF (Figure S8). It was not caused by the structural change of the Fmoc-FF nanofibers because they were known to be very stable under acidic conditions.[32] The morphology and optical property of the Fmoc-FF hydrogel was also maintained after the acid treatment, as shown in SEM images and PL spectrum (Figure S9). These results indicate that the interaction between the TPyP molecules and the Fmoc-FF nanofiber was mainly driven by electrostatic interaction, as depicted in Figure 1C. Although the kind of metal ions coordinated in the center of the TPyP monomers did not influence the formation of hydrogel, we only used SnTPyP in the

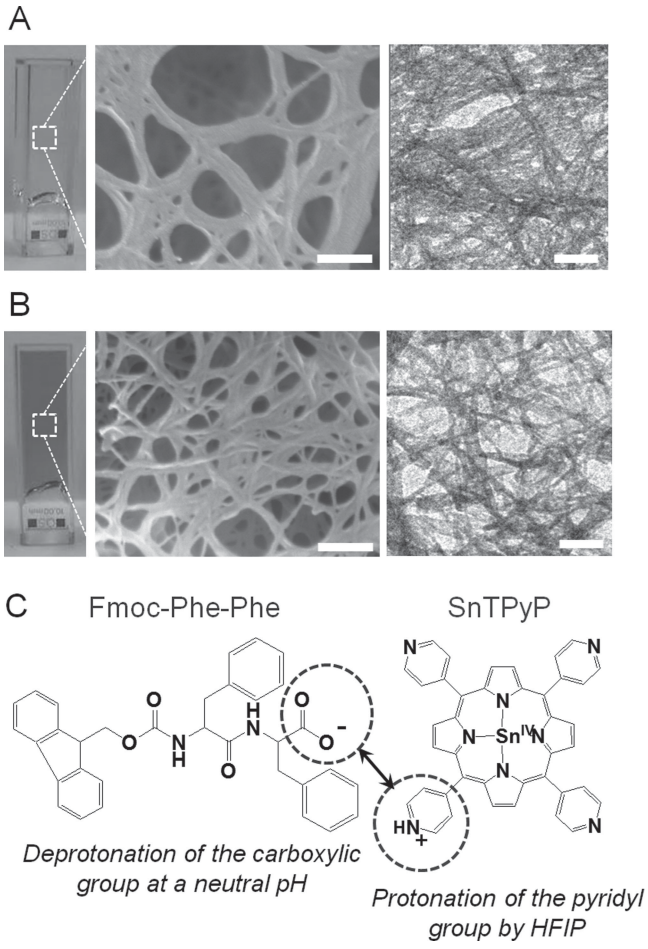

Figure 1. Photographs, SEM and TEM images of the (A) Fmoc-FF and (B) Fmoc-FF/SnTPyP hydrogel). The scale bar represents 200 nm. (C) Molecular structure of Fmoc-FF and SnTPyP. The Fmoc-FF peptides are negatively charged at a neutral pH owing to the deprotonation of the carboxylic group. In comparison to Fmoc-FF, SnTPyP has a cationic charge assisted by HFIP solution, as shown in Figure S6.

following section because SnTPyP has an oxidation potential of 1.1 V vs. NHE at pH 7.0, which is high enough for water oxidation, as shown in Figure S10 and Figure S11.

Next, we investigated the contribution of EET in the light-harvesting complexes to light-induced water oxidation. In natural photosystems, the enhanced exciton flux originates from the EET between the assembled chromophores, which are arranged closely with an average intermolecular distance of ≈ 8–10 Å.[34] The molecular structure of the Fmoc-FF nanofibers provides a close arrangement of the incorporated chromophores, facilitating EET. The proto-fibril of the Fmoc-FF nanofiber has a diameter of approximately 3 nm, as shown in **Figure 2**A, and the carboxylic groups on the Fmoc-FF nanofiber are positioned repetitively along the boundary lines of the region of the interlocking of fluorenyl groups with phenyl rings. To investigate whether the porphyrins in the Fmoc-FF hydrogel can mediate EET, we examined the optical properties of the Fmoc-FF/SnTPyP hydrogel using absorption and fluorescence spectroscopies. Both of the Soret and Q bands of SnTPyP were red-shifted when the SnTPyP molecules were incorporated into the Fmoc-FF hydrogel (Figure 2B). A slight blue shift of the Soret band was also observed in the Fmoc-FF/SnTPyP hydrogel. This phenomenon can be attributed to the formation of multiple types of aggregates, such as the H- and J-aggregates of SnTPyP, though the J-aggregation of SnTPyP molecules seems to be dominant.[35,36] The Soret band of the Fmoc-FF/TPyP hydrogel exhibited a broader spectral bandwidth, compared to that of the free SnTPyP monomers, which can be caused by the change of polarity around the assembled porphyrins.[37] In our case, various orientations of SnTPyP molecules may contribute to the broadening of the Soret band of SnTPyP because SnTPyP molecules are self-assembled with Fmoc-FF through multiple interactions (e.g., strong dipole-dipole interaction between the carboxylic group of Fmoc-FF and the pyridyl group of SnTPyP). In previous studies, the porphyrins assembled on the surface of M13 bacteriophages showed a similar broadening effect of the Soret band due to the molecular interactions of porphyrins with the amino acids of viral coat proteins.[38,39] Taken together, the red-shift and the broadening of the Soret-band indicate that the SnTPyP molecules were largely assembled into J-aggregates in the Fmoc-FF hydrogel.

The fluorescence spectra of the free SnTPyP monomers and Fmoc-FF/SnTPyP hydrogels were also compared to further examine the interactions between the SnTPyP molecules in the hydrogel. For the hydrogels, two different ratios of SnTPyP to Fmoc-FF, denoted R, were used at a fixed concentration of SnTPyP (0.2 μmol): R = 10 for Fmoc-FF/SnTPyP-1 and R = 5 for Fmoc-FF/SnTPyP-2. The fluorescence of SnTPyP was dramatically quenched in the Fmoc-FF/SnTPyP hydrogels (Figure 2C). The quenching effect was more significant at a higher ratio of SnTPyP to Fmoc-FF. These results indicate the existence of H-type coupling between the SnTPyP molecules incorporated within the hydrogel. The increased number of Fmoc-FF did not affect the molecular structure of the Fmoc-FF/SnTPyP hydrogel (Figure S12). The result suggests that the proximity of SnTPyP molecules caused the Dexter-type electronic interactions between the porphyrins, resulting in the formation of trap sites via orbital disordering.[34] Unfortunately, the precise determination and fine-tuning of the porphyrin-to-porphyrin distance could not be determined in this work due to the multiple interactions as described above. The control of the porphyrin-to-porphyrin distance is critically important for efficient EET. This might be the important limitation of our current system based on biomolecular self-assembly. Interestingly, the FRET emission from 700 nm to 850 nm was not observed in the Fmoc-FF/SnTPyP hybrid hydrogels, although the Stokes shift emission of Sn-containing porphyrins is possible over a similar wavelength range according to the literature.[40]

The fluorescence lifetimes of the free SnTPyP monomers and Fmoc-FF/SnTPyP hydrogels were also measured to further verify the energy transfer between the SnTPyP molecules self-assembled in the hydrogel. The fluorescence of the Fmoc-FF/SnTPyP-1 hydrogel decayed more quickly than those of the free SnTPyP monomers and Fmoc-FF/SnTPyP-2 hydrogel (**Figure 3**A). The lifetimes of the free SnTPyP monomers, Fmoc-FF/SnTPyP-1 hydrogel, and Fmoc-FF/SnTPyP-2 hydrogel were 1.38, 1.01, and 1.18 ns, respectively,

small NANO MICRO

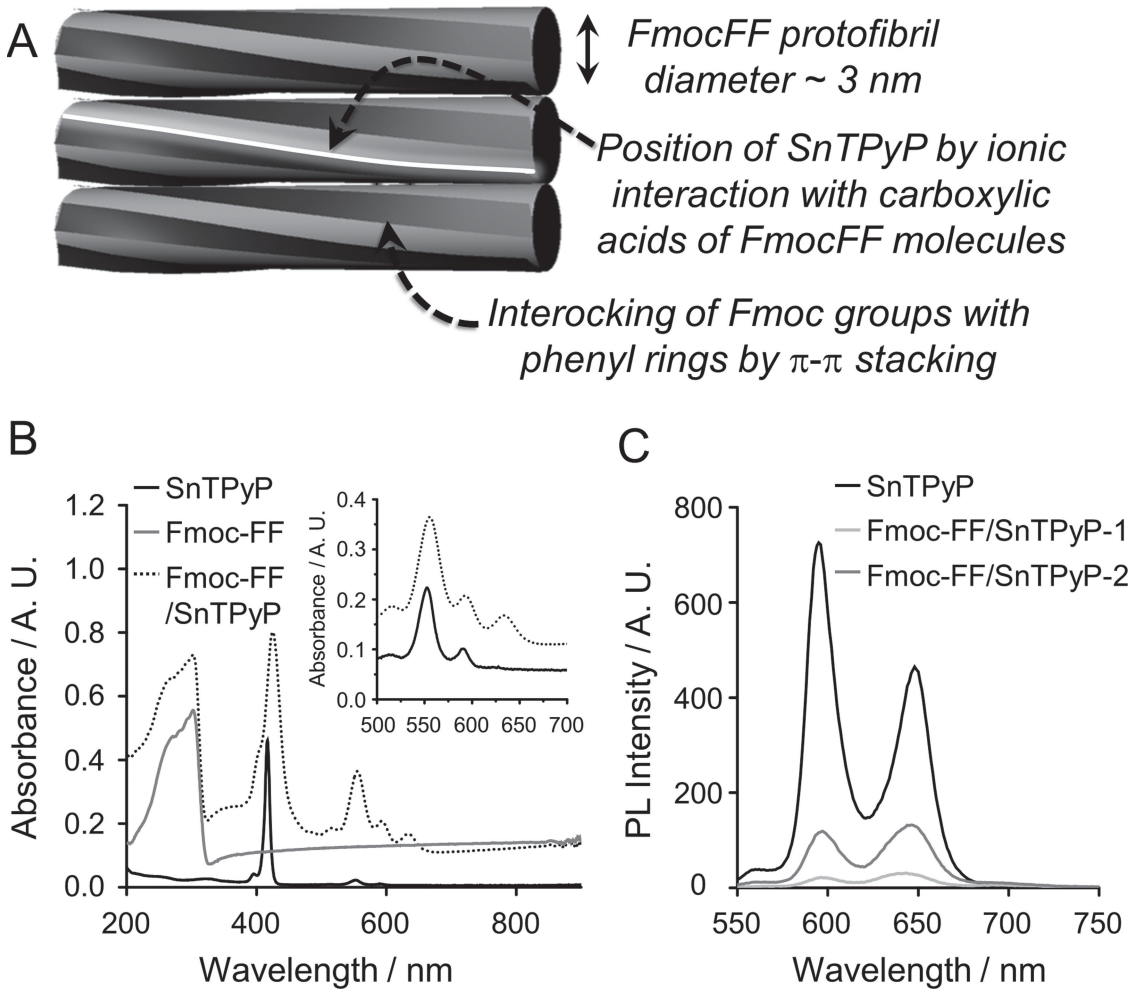

Figure 2. (A) Schematic description of a model structure of the Fmoc-FF hydrogel adapted from the literature.[28,33] The SnTPyP molecules were assembled on the carboxylic acids of the Fmoc-FF nanofiber, as depicted by the white line, which is positioned at the boundary of black and gray. (B) UV/vis spectra of the Fmoc-FF hydrogel (gray), free SnTPyP molecules (black), and Fmoc-FF/SnTPyP hydrogel (dotted black). The inset shows a magnified view of the UV/vis spectra of Q-bands (500 ~ 700 nm). (C) Emission spectra with excitation at 420 nm of the SnTPyP monomers (black), Fmoc-FF/SnTPyP-1 (light gray) and Fmoc-FF/SnTPyP-2 (dark gray). The spectroscopic analyses indicate that the SnTPyP molecules formed J-aggregates after incorporation into the Fmoc-FF hydrogel.

as determined using a double exponential function. The decreased lifetime of the Fmoc-FF/SnTPyP hydrogel is attributed to the EET between the assembled SnTPyP molecules.[41] We also measured the photocurrent of each material in a 0.1 M phosphate buffer at pH 8.0 (ionic strength ~ 0.29 M) containing 15 w/v% triethanolamine as an electron donor to observe photo-induced electron transfer. The net anodic photocurrent of the Fmoc-FF/SnTPyP-1 hydrogel was approximately three times higher than that of the Fmoc-FF/SnTPyP-2 hydrogel, indicating more effective light harvesting in the Fmoc-FF/SnTPyP-1 hydrogel (Figure 3B).

To investigate the effect of EET between SnTPyP molecules in the hydrogel on the efficiency of photochemical water oxidation, citrate-stabilized iridium oxide

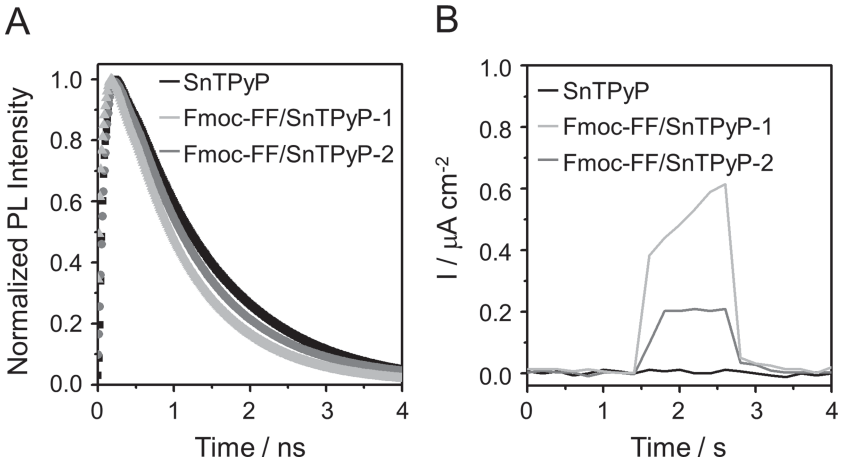

Figure 3. Emission decay profiles with excitation at 405 nm (A) and photocurrent (B) of the Fmoc-FF hydrogel or free SnTPyP molecules (black line), Fmoc-FF/SnTPyP-1 (light gray line), and Fmoc-FF/SnTPyP-2 (dark gray line). The J-aggregation of SnTPyP increased the rate of photo-induced electron transfer from the electron donor to acceptor because of EET between the SnTPyP molecules in the Fmoc-FF hydrogel.

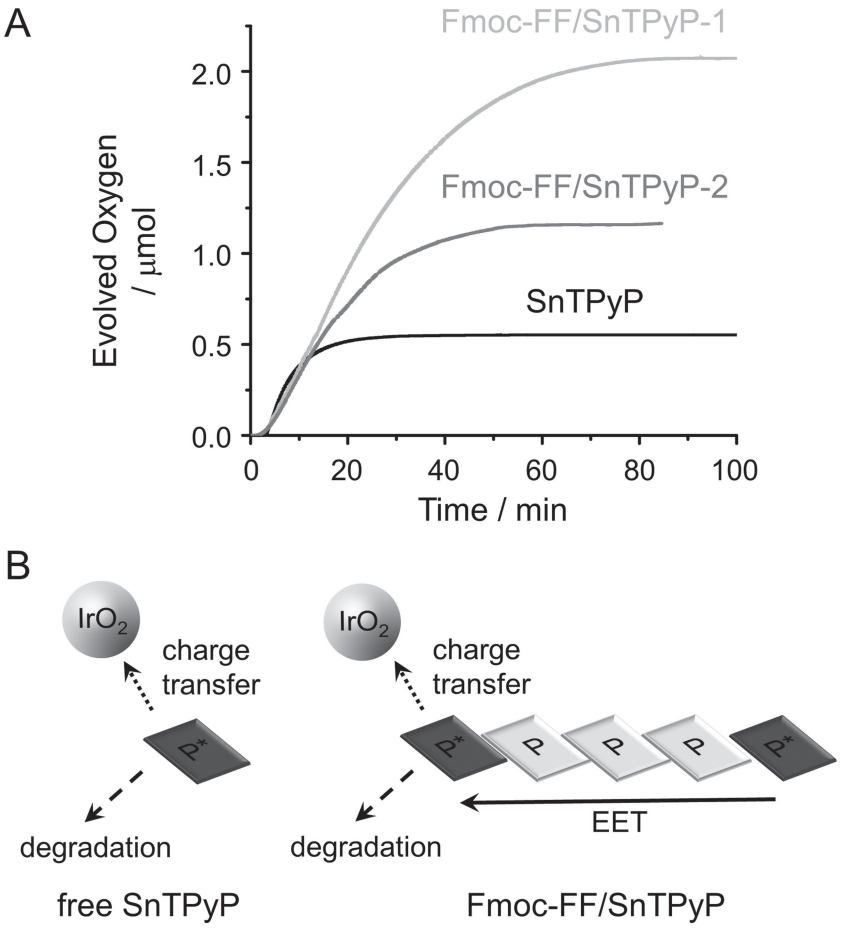

Figure 4. (A) Time-course oxygen production profiles for IrO_2 nanoparticles with 0.2 μmol SnTPyP molecules (black), Fmoc-FF/SnTPyP-1 (light gray), and Fmoc-FF/SnTPyP-2 (dark gray) in the 10 mL phosphate buffer at pH 7 containing 25 mM sodium persulfate. (B) A schematic illustration of the effect of EET on the catalytic activity of IrO_2 for photochemical water oxidation. The yellow and pink squares represent excited and ground states of SnTPyP, respectively.

(IrO_2) nanoparticles as a catalyst with the free SnTPyP monomers, Fmoc-FF/SnTPyP-1 hydrogel, and Fmoc-FF/SnTPyP-2 hydrogel. Oxygen evolution was monitored under the illumination of visible light ($\lambda > 420$ nm). Sodium persulfate ($Na_2S_2O_8$) was used as an electron acceptor in a 10 mM phosphate buffer at pH 7.0. The use of $Na_2S_2O_8$, an oxygen-containing electron acceptor, can complicate the measurement of the amount of evolved oxygen by Fmoc-FF/SnTPyP hydrogel with IrO_2 because the decomposition of S_2O_8 may liberate oxygen.[42,43] However, in our experimental condition at pH 7.0, S_2O_8 did not generate oxygen by its decomposition with water as shown in Figure S13. This result indicates that the oxygen evolution is mostly originated from water oxidation triggered by IrO_2 with Fmoc-FF/SnTPyP hydrogel. Only 0.55 μmol oxygen was produced with the free SnTPyP monomers (**Figure 4**A). On the contrary, approximately 2.0 μmol and 1.1 μmol of oxygen were generated per 0.11 mg of IrO_2 with the Fmoc-FF/SnTPyP-1 and Fmoc-FF/SnTPyP-2 hydrogels, respectively. Furthermore, the photochemical catalytic activity of the Fmoc-FF/SnTPyP hydrogels was maintained for about 1 h while the reaction with the free SnTPyP monomers did not proceed for any longer than 20 min. Accordingly, the turnover number was about 4.4 for the free SnTPyP monomers, 9.2 for the Fmoc-FF/SnTPyP-2 hydrogel, and 16.6 for the Fmoc-FF/SnTPyP-1 hydrogel, respectively. The saturated oxygen evolution originated from the degradation of SnTPyP by the formation of free radicals through the decomposition of the sacrificial electron acceptor. The similar phenomenon was also observed for IrO_2 with Zn(II) deuteroporphyrin IX 2,4 bis-ethyleneglycol was also observed due to the degradation of the porphyrins.[39] The turnover rate of IrO_2 was approximately 1.8×10^{-3} s^{-1} with the Fmoc-FF/SnTPyP-1 hydrogel, 1.5×10^{-3} s^{-1} with the Fmoc-FF/SnTPyP-2 hydrogel, and 2.1×10^{-3} s^{-1} free SnTPyP, respectively. This result indicates the significant role of EET induced in the Fmoc-FF nanofibers for photochemical water oxidation. Furthermore, an increased ratio of SnTPyP to Fmoc-FF can facilitate EET because of the closer distance between the SnTPyP molecules, as depicted in Figure 4B. The increased EET enhanced the stability of excited SnTPyP molecules in the Fmoc-FF hydrogel. The EET between the SnTPyPs assembled on the Fmoc-FF hydrogels inhibited the degradation pathway of excited SnTPyP through the creation of a new relaxation pathway. In the case of free SnTPyP, only relaxation pathway (charge transfer to IrO_2) exists. Thus, the SnTPyPs in the Fmoc-FF hydrogel were more stable than those in the free solution. Therefore, the higher catalytic activity of the Fmoc-FF/SnTPyP-1 hydrogel than that of the Fmoc-FF/SnTPyP-2 hydrogel and free SnTPyP monomers can be attributed to an increased flux of photon energy from water to an electron acceptor.

In summary, we introduced a light-harvesting hydrogel generated by the self-assembly of Fmoc-FF and porphyrins. The incorporation of the porphyrins into the hydrogel triggered EET, exhibiting a remarkable impact on the photochemical oxidation of water molecules by colloidal metal oxide catalysts. Both of the efficiency and duration of visible light-driven oxygen evolution dramatically increased via the EET of chromophores closely located within the light-harvesting hydrogel. Our study suggests that the well-defined molecular management of a light-harvesting process is essentially required to realize the ultimate aim of an artificial photosynthetic system. It is also suggested that the self-assembly of biomolecules is particularly attractive for creating a light-harvesting system capable of driving efficient EET as found in natural light-harvesting complexes. We expect that further investigation on biomolecular self-assembly will eventually provide the precise control of the distance and orientation of the assembled chromophores and their chemical microenvironments, all of which are critically important for EET.

NANO MICRO small

Supporting Information

Supporting Information is available from the Wiley Online Library or from the author.

Acknowledgements

This study was supported by grants from the National Research Foundation (NRF) via Converging Research Center (2009–0082276), National Research Laboratory (R0A-2008–000–20041–0), and Intelligent Synthetic Biology Center of Global Frontier Project (2011–0031957), Republic of Korea.

[1] H. B. Gray, *Nature Chem.* **2009**, *1*, 7.
[2] J. Barber, *Chem. Soc. Rev.* **2009**, *38*, 185.
[3] R. Abe, *J. Photochem. Photobiol., C* **2010**, *11*, 179.
[4] K. Kalyanasudaram, M. Graetzel, *Curr. Opin. Biotechnol.* **2010**, *21*, 298.
[5] S. H. Lee, J. H. Kim, C. B. Park, *Chem. Eur. J.* **2013**, *19*, 3492.
[6] T. E. Mallouk, *J. Phys. Chem. Lett.* **2010**, *1*, 2738.
[7] R. Cao, W. Lai, P. Du, *Energy Enviorn. Sci.* **2012**, *5*, 8134.
[8] E. Collini, C. Y. Wong, K. E. Wilk, P. M. G. Curmi, P. Brumer, G. D. Scholes, *Nature* **2010**, *463*, 644.
[9] M. R. Wasielewski, *Acc. Chem. Res.* **2009**, *42*, 1910.
[10] J. Iehl, J.-F. Nierengarten, A. Harriman, T. Bura, R. Ziessel, *J. Am. Chem. Soc.* **2012**, *134*, 988.
[11] A. C. Benniston, A. Harriman, *Mater. Today* **2008**, *11*, 26.
[12] C. She, S. J. Lee, J. E. McGarrah, J. Vura-Weis, M. R. Wasielewski, H. Chen, G. C. Schatz, M. A. Ratner, J. T. Hupp, *Chem. Commun.* **2010**, *46*, 547.
[13] G. D. Scholes, G. R. Fleming, A. Olaya-Castro, R. Van Grondelle, *Nat. Chem.* **2011**, *3*, 763.
[14] J. Ryu, S. Y. Lim, C. B. Park, *Adv. Mater.* **2009**, *21*, 1577.
[15] J. H. Kim, M. Lee, J. S. Lee, C. B. Park, *Angew. Chem. Int. Ed.* **2012**, *124*, 532.
[16] B. D. Wall, S. R. Diegelmann, S. Zhang, T. J. Dawidczyk, W. L. Wilson, H. E. Katz, H.-Q. Mao, J. D. Tovar, *Adv. Mater.* **2011**, *23*, 5009.
[17] E.-K. Schillinger, E. Mena-Osteritz, J. Hentschel, H. G. Börner, P. Bäuerle, *Adv. Mater.* **2009**, *21*, 1562.
[18] M. Reches, E. Gazit, *Science* **2003**, *300*, 625.
[19] J. Ryu, C. B. Park, *Adv. Mater.* **2008**, *20*, 3754.
[20] L. Adler-Abramovich, E. Gazit, *J. Pept. Sci.* **2008**, *14*, 217.
[21] J. Ryu, S.-W. Kim, K. Kang, C. B. Park, *Adv. Mater.* **2010**, *22*, 5537.
[22] J. Ryu, C. B. Park, *Adv. Mater.* **2009**, *48*, 4820.
[23] R. Huang, W. Qi, L. Feng, R. Su, Z. He, *Soft Matter* **2011**, *7*, 6222.
[24] N. Amdursky, E. Gazit, G. Rosenman, *Adv. Mater.* **2010**, *22*, 2311.
[25] J. Ryu, C. B. Park, *Biotechnol. Bioeng.* **2010**, *105*, 221.
[26] M. Yemini, M. Reches, J. Rishpon, E. Gazit, *Nano Lett.* **2005**, *5*, 183.
[27] C. Tang, R. V. Ulijn, A. Saiani, *Langmuir* **2011**, *27*, 14438.
[28] A. M. Smith, R. J. Williams, C. Tang, P. Coppo, R. F. Collins, M. L. Turner, A. Saiani, R. V. Ulijn, *Adv. Mater.* **2008**, *20*, 37.
[29] C. Tang, A. M. Smith, R. F. Collins, R. V. Ulijn, A. Saiani, *Langmuir* **2009**, *25*, 9447.
[30] D. A. Skoog, D. M. West, F. J. Holler, S. R. Crouch, *Fundamental of Analytic Chemistry*, 5th edition, New York: Saunders College Publishing. **1988**, Ch. 8.
[31] I. Kulszewicz-Bajer, *Synth. Met.* **1997**, *30*, 7091.
[32] J. Raeburn, G. Pont, L. Chen, Y. Cesbron, R. Lévy, D. J. Adams, *Soft Matter* **2012**, *8*, 1168.
[33] M. Zhou, A. M. Smith, A. K. Das, N. W. Hodson, R. F. Collins, R. V. Ulijn, J. E. Gough, *Biomaterials* **2009**, *30*, 2523.
[34] D. Noy, *Photosynth. Res.* **2008**, *95*, 23.
[35] R. F. Khairutdinov, N. Serpone, *J. Phys. Chem. B* **1999**, *103*, 761.
[36] S. Okada, H. Segawa, *J. Am. Chem. Soc.* **2003**, *125*, 2792.
[37] D. Mauzerall, *Biochemistry* **1965**, *4*, 1801.
[38] Y. S. Nam, T. Shin, H. Park, A. P. Magyar, K. Choi, G. Fantner, K. A. Nelson, A. M. Belcher, *J. Am. Chem. Soc.* **2010**, *132*, 1462.
[39] Y. S. Nam, A. P. Magyar, D. Lee, J.-W. Kim, D. S. Yun, H. Park, T. S. Pollom Jr., D. A. Weitz, A. M. Belcher, *Nat. Nanotechnol.* **2010**, *5*, 340.
[40] N. Venkatramaiah, B. Ramakrishna, A. R. Kumar, N. Veeraiah, R. Venkatesan, *J. Alloy. Compd.* **2012**, *513*, 318.
[41] L. Valkunas, J. Chmeliov, G. Trinkunas, C. D. P. Duffy, R. Van Grondelle, A. V. Ruban, *J. Phys. Chem. B* **2011**, *115*, 9252.
[42] I. M. Kolthoff, I. K. Miller, *J. Am. Chem. Soc.* **1951**, *73*, 3055–3059.
[43] A. Magnuson, H. Berglund, P. Korall, L. Hammarström, B. Åkermark, S. Styring, L. Sun, *J. Am. Chem. Soc.* **1997**, *119*, 10720.

Received: August 12, 2013
Revised: September 6, 2103
Published online: November 8, 2013

